

Article

A New Indicator to Better Represent the Impact of Landscape Pattern Change on Basin Soil Erosion and Sediment Yield in the Upper Reach of Ganjiang, China

Yongfen Zhang ^{1,2}, Nong Wang ², Chongjun Tang ², Shiqiang Zhang ^{1,*}, Yuejun Song ², Kaitao Liao ^{2,3} and Xiaofei Nie ^{2,4}

¹ College of Urban and Environmental Science, Northwest University, Xi'an 710127, China; yongfenyk@stumail.nwu.edu.cn

² Jiangxi Provincial Key Laboratory of Soil Erosion and Prevention, Jiangxi Academy of Water Science and Engineering, Nanchang 330029, China; house_e@163.com (N.W.); tangchongjun@126.com (C.T.); well3292@126.com (Y.S.); liaokaitao@jxnu.edu.cn (K.L.); xfnie85@163.com (X.N.)

³ School of Geography and Environment, Jiangxi Normal University, Nanchang 330027, China

⁴ Research Center of Soil and Water Conservation and Ecological Environment, Chinese Academy of Sciences and Ministry of Education, Xianyang 712100, China

* Correspondence: zhangsq@nwu.edu.cn



Citation: Zhang, Y.; Wang, N.; Tang, C.; Zhang, S.; Song, Y.; Liao, K.; Nie, X. A New Indicator to Better Represent the Impact of Landscape Pattern Change on Basin Soil Erosion and Sediment Yield in the Upper Reach of Ganjiang, China. *Land* **2021**, *10*, 990. <https://doi.org/10.3390/land10090990>

Academic Editor: Cezary Kabala

Received: 1 August 2021

Accepted: 17 September 2021

Published: 19 September 2021

Publisher's Note: MDPI stays neutral with regard to jurisdictional claims in published maps and institutional affiliations.



Copyright: © 2021 by the authors. Licensee MDPI, Basel, Switzerland. This article is an open access article distributed under the terms and conditions of the Creative Commons Attribution (CC BY) license (<https://creativecommons.org/licenses/by/4.0/>).

Abstract: Landscape patterns are a result of the combined action of natural and social factors. Quantifying the relationships between landscape pattern changes, soil erosion, and sediment yield in river basins can provide regulators with a foundation for decision-making. Many studies have investigated how land-use changes and the resulting landscape patterns affect soil erosion in river basins. However, studies examining the effects of terrain, rainfall, soil erodibility, and vegetation cover factors on soil erosion and sediment yield from a landscape pattern perspective remain limited. In this paper, the upper Ganjiang Basin was used as the study area, and the amount of soil erosion and the amount of sediment yield in this basin were first simulated using a hydrological model. The simulated values were then validated. On this basis, new landscape metrics were established through the addition of factors from the revised universal soil loss equation to the land-use pattern. Five combinations of landscape metrics were chosen, and the interactions between the landscape metrics in each combination and their effects on soil erosion and sediment yield in the river basin were examined. The results showed that there were highly similar correlations between the area metrics, between the fragmentation metrics, between the spatial structure metrics, and between the evenness metrics across all the combinations, while the correlations between the shape metrics in Combination 1 (only land use in each year) differed notably from those in the other combinations. The new landscape indicator established based on Combination 4, which integrated the land-use pattern and the terrain, soil erodibility, and rainfall erosivity factors, were the most significantly correlated with the soil erosion and sediment yield of the river basin. Finally, partial least-squares regression models for the soil erosion and sediment yield of the river basin were established based on the five landscape metrics with the highest variable importance in projection scores selected from Combination 4. The results of this study provide a simple approach for quantitatively assessing soil erosion in other river basins for which detailed observation data are lacking.

Keywords: landscape metrics; soil erosion; sediment yield; PLSR

1. Introduction

As a comprehensive reflection of the ecological-environmental system in a region, the landscape pattern is a spatial arrangement of different landscape mosaics that results from the interaction of multiple natural and human factors [1,2]. Changes in the spatial distribution of the landscape pattern can affect the water cycle and therefore soil erosion

and sediment yield in a region [3,4]. Hence, studying the response of the water and sediment processes to landscape pattern changes in a river basin from a landscape ecology perspective can to some extent reveal the effects of changes in natural conditions and human activity on the water and sediment in the river basin [5–7]. Land use—an important component of a landscape—primarily acts on the vegetation landscape pattern and processes such as hydrological flow. The spatial land-use pattern has notable impacts on runoff, soil erosion, and sediment yield at different scales [8]. Hence, many studies have focused on the correlations between land-use-derived landscape metrics and the amount of soil erosion and the amount of sediment yield [9–16]. Partial least-squares regression (PLSR) is a new technique that combines principal component analysis (PCA) and multiple linear regression (MLR). PLSR is an important tool for quantitatively studying the relationships between landscape metrics and soil erosion and sediment yield in river basins [9,17,18].

Soil erosion and sediment yield in a river basin are comprehensive processes. In the investigation of factors related to soil erosion and sediment yield in a river basin, it may be insufficient to consider only the landscape metrics that are specific to the land use because this neglects the effects of factors such as terrain, soil, and rainfall on the hydrological processes in the river basin. Therefore, several models have been developed to assess soil erosion and sediment yield, among which the revised universal soil loss equation (RUSLE) has been extensively used worldwide to estimate soil erosion at the watershed scale due to its simple structure, easy-to-acquire parameters, simple calculations, and consideration of the main factors affecting soil erosion, as well as its ability to predict erosion more accurately [19–23]. It has been widely used in the estimation of soil erosion at the basin scale worldwide. Hence, in this study, the slope gradient and aspect (LS), the rainfall erosivity (R), the soil erodibility (K), and the vegetation cover (C) factors in the RUSLE were combined with the land use to establish new landscape patch units, whose relationships with soil erosion and sediment yield in a river basin were then quantified. The results of this study provide a new approach to exploring and developing quantitative relationships between landscape metrics and soil erosion and sediment yield in river basins.

The upper Ganjiang Basin once suffered from severe soil erosion problems [24]. Considerable efforts (e.g., afforestation, as well as water and soil conservation facility construction) made to mitigate soil erosion in this region since the 1980s have significantly changed its natural and social conditions and notably reduced soil erosion and the amount of sediment transported into the river [25]. These conditions provide an excellent case for conducting this study, which has the following main objectives: (1) to establish a soil and water assessment tool (SWAT) model for the upper Ganjiang Basin, as well as correct and validate it based on measured monthly runoff and sediment discharge data; (2) to design multiple combinations of landscape metrics and compare the correlations between these metrics at different sub-river basins and between these landscape metrics and the soil erosion and sediment yield in the different combinations; and (3) to quantify the correlations between the landscape metrics selected from the combination with the strongest correlations and the soil erosion and sediment yield in the river basin based on PLSR models.

2. Materials and Methods

2.1. Study Area

The upper Ganjiang Basin is located between 113°30' E–116°40' E and 24°26' N–27°07' N (Figure 1). The basin experiences a subtropical monsoonal humid climate with an annual precipitation of 1400–2000 mm, which shows obvious interannual variation and uneven distribution throughout the year. The flood season is from April to September of each year. The precipitation during this period accounts for 65% to 70% of the total annual precipitation. The average temperature throughout the year is 17–26 °C. The rocks composing the stratigraphy of the upper Ganjiang Basin mainly include sedimentary, magmatic, and metamorphic rocks. Granite is a typical representative of magmatic rocks in the basin. The main soil type is Acrisols, which is an acidic soil that is rich in iron and aluminum

oxides and which forms in humid climates [26]. The terrain in this area is dominated by low mountains and hills [27].

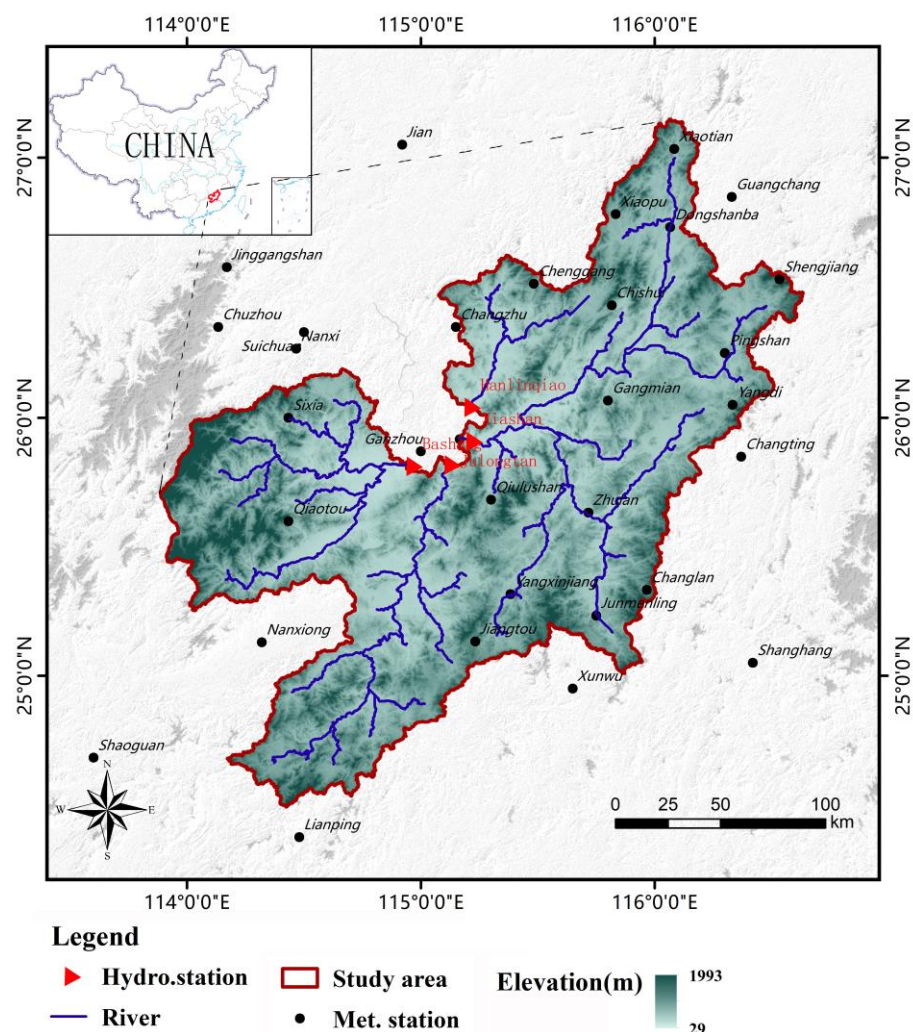


Figure 1. The position of the upper Ganjiang Basin.

2.2. SWAT Model Simulations

The SWAT model has been widely used in studies in different parts of the world [28–33]. It provides a simulation of the hydrology and associated material transport transformations in a watershed by integrating the watershed topography, soils, land-use, weather, and land-management practices [32]. The meteorological data involved in the construction of the SWAT model were collected from 32 meteorological (rainfall) stations around the upper Ganjiang Basin from 1975 to 2010. Daily precipitation, maximum/minimum temperature, relative humidity, and wind speed data for 12 meteorological stations were collected from the China Meteorological Data Service Center (<http://data.cma.cn> (accessed on 11 April 2019)). Daily precipitation data for 30 rainfall stations were collected from the Jiangxi Hydrology Bureau (Figure 1). The ASTER GDEM dataset (30 m × 30 m) was supplied by the Geospatial Data Cloud site, Computer Network Information Center, Chinese Academy of Sciences (<http://www.gscloud.cn>, accessed on 7 April 2017). The 1980, 1995, and 2010 land-use data (30 m × 30 m) were obtained from the Resource and Environment Data Cloud Platform, Chinese Academy of Sciences (<http://www.resdc.cn>, accessed on 19 September 2016) (Figure 2). Based on the input data requirements of the SWAT model, the three periods of land-use data were reclassified by merging similar land-use types. The reclassified land-use types included paddy, upland, forest, shrubland, open forest, garden, grassland, and construction land (Figure 2). The Harmonized World Soil Database

(HWSD_v121) in SWAT format (1 km × 1 km) was obtained from the Water Weather Energy Ecosystem Technology and Data website, 2w2e GmbH (<https://www.2w2e.com/>, accessed on 16 December 2018). Monthly flow data for the four hydrological stations at Hanlinqiao, Xiashan, Julongtan, and Bashang were obtained from the Jiangxi Provincial Hydrological Bureau (Figure 1).

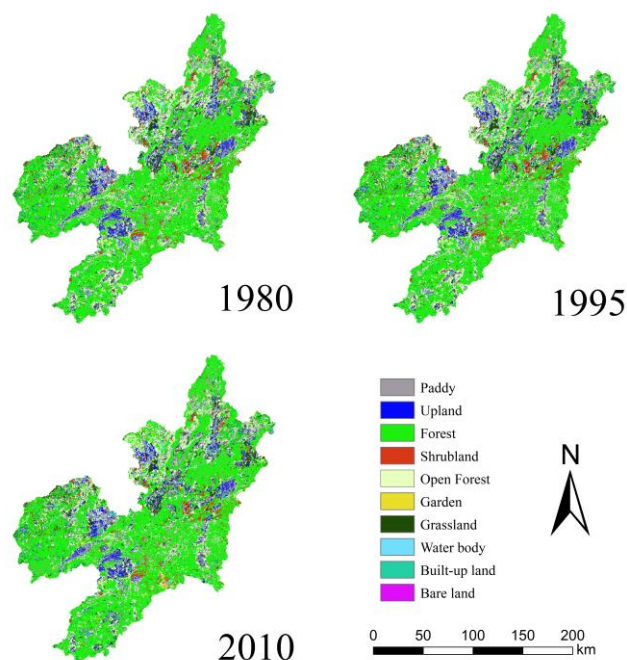


Figure 2. Land-use distribution in the upper Ganjiang Basin, 1980, 1995, and 2010.

The sequential uncertainty fitting (SUFI-2) method in the SWAT Calibration and Uncertainty Program (CUP) was used for model calibration and validation using the P-factor and R-factor to measure the effects of model rate-setting and uncertainty analysis [30,34]. The P-factor represents the percentage of observed data enveloped by the modeling result, the 95 PPU (95% prediction uncertainty), and the R-factor represents the mean width of the 95 PPU interval divided by the standard deviation of the measured data. In general, the closer the P-factor is to 1 and the closer the R-factor is to 0, the closer the simulation is to the true value. The uncertainty of the simulation is considered acceptable when the P-factor > 0.5 and R-factor < 1.5; when the P-factor > 0.7 and R-factor < 1, the uncertainty of the simulation is low [30]. The coefficient of determination (R^2) and the Nash–Sutcliffe coefficient (NS) were used in this paper to evaluate the applicability of the SWAT model. R^2 indicates the consistency of the trends between the simulated and measured values. A value closer to 1 means that the simulated values are more consistent with the measured values. $R^2 > 0.6$ is usually used as a criterion for the degree of correlation between measured and simulated values. NS indicates the degree of the deviation of the measured value from the simulated value. The closer the value is to 1, the smaller the deviation between the simulated and measured values. When $NS \leq 0.36$, the simulation is considered to be unsatisfactory. When $0.36 < NS < 0.75$, the simulation is considered to be good. When $NS \geq 0.75$, the simulation is considered to be excellent [35].

2.3. Partial Least-Squares Regression

PLSR is a robust multiple regression technique that can be used to establish regression models when there are significant multiple correlations between the independent variables. By combining the features of PCA and MLR, the PLSR technique can produce modeling analyses with higher reliability and integrity [36]. In this study, the landscape metrics were treated as independent variables, while the soil erosion and sediment yield in each sub-river basin were set as dependent variables. To establish models with both high predictive

performance and high stability, a suitable combination of components is generally arrived at for each PLSR model through cross-validation to achieve an optimal balance between the explained variability in the response (R^2) and the predictive ability of the model (Q^2). It is generally considered that a model with a cumulative Q^2 (Q^2_{cum}) greater than 0.5 has a high predictive ability. The root mean square error of cross-validation (RMSECV) can be used to determine the difference between predicted and observed values. The importance of a predictor variable to the independent and dependent variables is given by the variable importance in projection (VIP) score. Terms with high VIP scores are the most strongly correlated with the dependent (explained) variables. See references for the detailed correlation algorithm and theory [18,36]. In this study, SIMCA-P software was used to establish PLSR models, and SPSS 20 was used to evaluate the correlations between the landscape metrics and between each landscape metric and the soil erosion and sediment yield in each sub-river basin.

2.4. Design of Combinations

In this study, the land use in each year was combined with the LS factor, the K factor, the C factor for each year, and/or the R factor in the RUSLE to form new landscape patch units. Then, the landscape metrics were calculated. Based on the SWAT-calculated and validated soil erosion and sediment yield data for each sub-river basin, the correlations between the landscape metrics and between each landscape metric and soil erosion and sediment yield in different combinations were compared. On this basis, the combination with the strongest correlations was selected to quantify the correlations between the landscape metrics and soil erosion and sediment yield. The following combinations were designed to calculate the landscape metrics.

Combination 1: land use in each year.

Combination 2: land use in each year + LS + K.

Combination 3: combination 2 + C.

Combination 4: combination 2 + R.

Combination 5: combination 2 + C + R.

Here, the land-use data that were used to establish the SWAT model were used for analysis. See the literature [37] for the data sources and calculation methods for the LS, K, C, and R factors, which were derived from existing research results.

Of the above-mentioned factors in the RUSLE, the LS and K factors were unlikely to have changed significantly over the time period selected for analysis in this study and thus were considered to have remained relatively unchanged, whereas the C and R factors varied with time. Therefore, Combination 1 was calculated as the conventional landscape metric. From this, Combination 2 was established by adding the fixed LS and K factors to Combination 1, while Combination 3, Combination 4, and Combination 5 were established by adding the C factor, the R factor, and both C and R to Combination 2, respectively, with the goal of distinguishing the possible correlations between the landscape metrics that arose from the respective addition of the fixed and dynamic factors and the soil erosion and sediment yield in the river basin.

To comprehensively reflect the landscape pattern features of the river basin and to reduce redundant information, 17 landscape-scale metrics (i.e., the patch density (PD), the largest patch index (LPI), the mean patch area (AREA_MN), the edge density (ED), the mean nearest-neighbor distance (ENN_MN), the landscape shape index (LSI), the mean shape index (SHAPE_MN), the mean perimeter–area ratio (PARA_MN), the perimeter–area fractal dimension (PAFRAC), the contagion index (CONTAG), the interspersion and juxtaposition index (IJI), the division index (DIVISION), the splitting index (SPLIT), the aggregation index (AI), Shannon’s diversity index (SHDI), Simpson’s diversity index (SIDI), and Shannon’s evenness index (SHEI)) were selected based on previous research and were calculated by FRAGSTATS 4.2. See relevant references [38,39] for the calculation methods and ecological meanings of these landscape metrics.

3. Results

3.1. Model Calibration and Validation

Due to the uncertainty of the SWAT model parameters, if the simulation is carried out over an extremely long time series, the effect of long-term changes in land-use patterns on the hydrological process will be eliminated, generating pseudoparameters that will affect the accuracy of the simulation results [35]. At the same time, since the data that can be collected were limited, we can only perform simulations and validations for the time period 1980–2010. Therefore, this study conducted scenario simulations for three separate time periods—1980, 1995, and 2010—and the calibration and validation periods were as close to 1980, 1995, and 2010 as possible. Specifically, (1) for the land-use scenario in 1980, the periods 1977–1979, 1980–1982, and 1983–1985 were set as the warm-up, calibration, and validation periods, respectively; (2) for the land-use scenario in 1995, the periods 1990–1992, 1993–1995, and 1996–1998 were set as the warm-up, calibration, and validation periods; and (3) for the land-use scenario in 2010, the periods 2002–2004, 2005–2007, and 2008–2010 were set as the warm-up, calibration, and validation periods.

Based on previous findings, 16 runoff sensitivity [27] and 5 sediment discharge sensitivity parameters (Table 1) were determined and selected in this study to further calibrate the model for each sub-river basin. Then, based on the monthly runoff and sediment discharge data measured at four hydrological stations (i.e., the Hanlinqiao, Xiashan, Bashang, and Julongtan stations) in the periods 1980–1985 (P_{1980s}), 1993–1998 (P_{1995s}), and 2005–2010 (P_{2010s}), the sequential uncertainty fitting 2 (SUFI-2) algorithm in the SWAT calibration uncertainty program was used to analyze the uncertainty of the output of the SWAT model at each relevant sub-river basin, as well as to calibrate and validate the SWAT model. The results showed the following.

Table 1. The parameters for model calibration and validation and their maximum theoretical range.

Parameter	Description	Maximum Theoretical Range
PRF	Peak rate adjustment factor for sediment routing	0–2
CH_COV	Channel cover factor	−0.001–1
CH_EROD	Channel erodibility factor	−0.05–0.6
SPCON	Linear parameters for calculating the channel sediment routing	0.0001–0.01
SPEXP	Exponent parameter for calculating the channel sediment routing	1–2

The SWAT model was well-calibrated for the runoff at all four hydrological stations [27]. There was a very low degree of uncertainty in the simulated sediment at each of the four hydrological stations (Table 2). In both the calibration and validation periods, the R^2 values for the four hydrological stations in the three historical scenarios were greater than 0.6, suggesting a strong correlation between the trends of the simulated and measured values. The Nash–Sutcliffe (NS) coefficient was above 0.5 for the Hanlinqiao and Xiashan stations for each period, indicating that the quality of the simulated values ranged from good to excellent. The NS coefficient was above 0.36 for the Julongtan station in P_{1980s} and P_{1995s} , indicating that the simulated values were acceptable. However, the NS coefficient was low for the Julongtan station in the calibration period of P_{2010s} . For the Bashang station, the NS coefficient ranged from 0.73 to 0.89 in P_{1980s} and from 0.72 to 0.73 in the calibration periods of both P_{1995s} and P_{2010s} , suggesting that the simulated values were good. However, the simulated values for the Bashang station in the validation periods were unsatisfactory. Overall, the performance of the SWAT model in simulating the runoff and sediment in the upper Ganjiang Basin in each period varied. The SWAT model displayed good performance in simulating runoff, whereas its simulation accuracy for sediment in some sub-river basins in the validation periods of P_{1995s} and P_{2010s} was low. Nevertheless,

the trends of the simulated values generated by the SWAT model were close to those of the measured values. Hence, the SWAT model could be used for further analysis.

Table 2. Results of uncertainty analyses and evaluations of the sediment simulations under three historical scenarios—1980, 1995, and 2010—at each hydrological station.

Station	Land-Use Scenario	Calibration & Validation	P-Factor	R-Factor	R ²	NS
Hanlinqiao	1980	Calibration (1980–1982)	0.54	0.45	0.87	0.54
		Validation (1983–1985)	—	—	0.82	0.59
	1995	Calibration (1993–1995)	0.78	0.9	0.73	0.7
		Validation (1996–1998)	—	—	0.76	0.61
	2010	Calibration (2005–2007)	0.89	0.77	0.85	0.8
		Validation (2008–2010)	—	—	0.92	0.75
Xiashan	1980	Calibration (1980–1982)	0.82	0.86	0.93	0.9
		Validation (1983–1985)	—	—	0.87	0.86
	1995	Calibration (1993–1995)	0.92	0.97	0.86	0.79
		Validation (1996–1998)	—	—	0.92	0.64
	2010	Calibration (2005–2007)	0.99	0.97	0.92	0.71
		Validation (2008–2010)	—	—	0.93	0.7
Julongtan	1980	Calibration (1980–1982)	0.61	1.08	0.85	0.77
		Validation (1983–1985)	—	—	0.83	0.62
	1995	Calibration (1993–1995)	0.89	1.07	0.85	0.81
		Validation (1996–1998)	—	—	0.86	0.38
	2010	Calibration (2005–2007)	0.76	1.88	0.65	0.61
		Validation (2008–2010)	—	—	0.81	−7.11
Bashang	1980	Calibration (1980–1982)	0.97	1.01	0.91	0.89
		Validation (1983–1985)	—	—	0.76	0.73
	1995	Calibration (1993–1995)	0.83	1.76	0.76	0.73
		Validation (1996–1998)	—	—	0.84	−3.73
	2010	Calibration (2005–2007)	0.99	1.2	0.8	0.72
		Validation (2008–2010)	—	—	0.77	−3.97

3.2. Analysis of Land Use, Soil Erosion, and Sediment Yield Changes

A comparison of the land-use types in the upper Ganjiang Basin at the three time points showed no significant change in the proportion of the total land area used for each land-use type (Table 3, Figure 2). Specifically, paddy fields, dry lands, forests, shrublands, open forests, other wooded lands, grasslands, water bodies, and construction lands accounted for 11.53–11.66%, 6.5–6.77%, 2.25–53.72%, 3.36–3.92%, 15.63–17.80%, 0.32–1%, 5.79–6.02%, 0.89–0.92%, and 0.88–1.16% of the total land area, respectively.

Table 3. Land-use changes in the upper Ganjiang Basin, 1980, 1995, and 2010.

	1980 (km ²)	1995 (km ²)	2010 (km ²)
Paddy	3889	3847	3883
Upland	2184	2170	2258
Forest	17,429	17,498	17,919
Shrubland	1241	1306	1120
Open forest	5936	5795	5213
Garden	118	106	335
Grassland	1965	2009	1931
Water body	298	291	306
Built-up land	292	331	388
Bare land	3	2	2

However, a horizontal comparison of the area of each land-use type among the three time points reveals some notable changes. The area of paddy fields was 1.08% smaller in 1995 than in 1980 but recovered in 2010 to 99.85% of the reference level. The area of

dry lands was 0.64% smaller in 1995 than in 1980 but recovered rapidly and surpassed the reference level by 3.39% in 2010. The area of forests increased: it was 0.40% and 2.81% larger in 1995 and 2010 than in 1980, respectively. The area of shrublands was 5.24% larger in 1995 than in 1980, after which it decreased rapidly to 9.75% smaller in 2010 than in 1980. The area of open forests continuously decreased: it was 2.38% and 12.18% lower in 1995 and 2010 than in 1980, respectively. The area of other wooded lands first decreased and then increased at an extremely high rate. Specifically, compared to 1980, the area of other wooded lands was 10.17% smaller in 1995 but was 183.90% larger in 2010. Of all the land-use types, the area of other wooded lands increased by the greatest percentage and thus warrants close attention. The area of grasslands first increased and then decreased. The area of water bodies first decreased and then increased with a narrow range with $\pm 7 \text{ km}^2$ over 30 years. Construction lands are another land-use type that merits attention. Compared to 1980, the area of construction lands was 13.36% larger in 1995, and this number increased to 32.88% in 2010.

An observation of the spatial distribution maps of the soil erosion and sediment yield in the river basin during the three periods reveals a notable decline in both the soil erosion and sediment yield (Figures 3 and 4). The average soil erosion modulus decreased from 92.63 t/ha/yr in P_{1980s} to 72.92 t/ha/yr in P_{1995s} and further to 37.88 t/ha/yr in P_{2010s}, translating to a rate of decrease of 21.28% and 59.11%, respectively. The average sediment yield decreased from 36.23 t/ha/yr in P_{1980s} to 26.61 t/ha/yr in P_{1995s} and to 12.70 t/ha/yr in P_{2010s}, translating to a rate of decrease of 26.55% and 64.95%, respectively (Table 4).

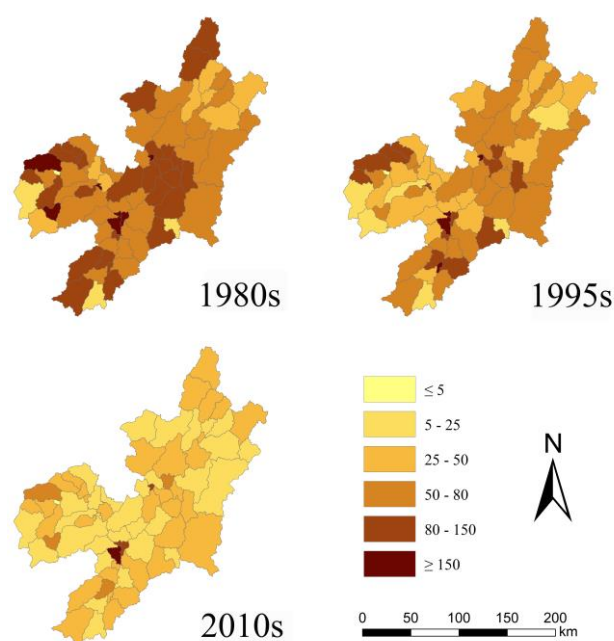


Figure 3. Soil erosion distribution of each sub-basin for the years 1980s, 1995s, and 2010s (t/ha/yr).

The distribution patterns of the soil erosion in different years were similar. An analysis of the distribution maps of the soil erosion and sediment yield in conjunction with the regional terrain and land-use maps shows the following. Generally, the soil erosion was higher in hilly areas with fragmented terrain and smaller in river valleys with flat terrain. The soil erosion was higher in areas where uplands and construction lands accounted for more of the sub-river basin and lower in areas where forests and grasslands accounted for more of the sub-river basin. In addition, the sediment yield was correspondingly high in the high-soil erosion areas. However, except for the upper reaches of each tributary, the sediment yield was notably low in the valleys through which the Ganjiang runs. This phenomenon also reflects the role of flat terrain in intercepting sediment produced by soil erosion.

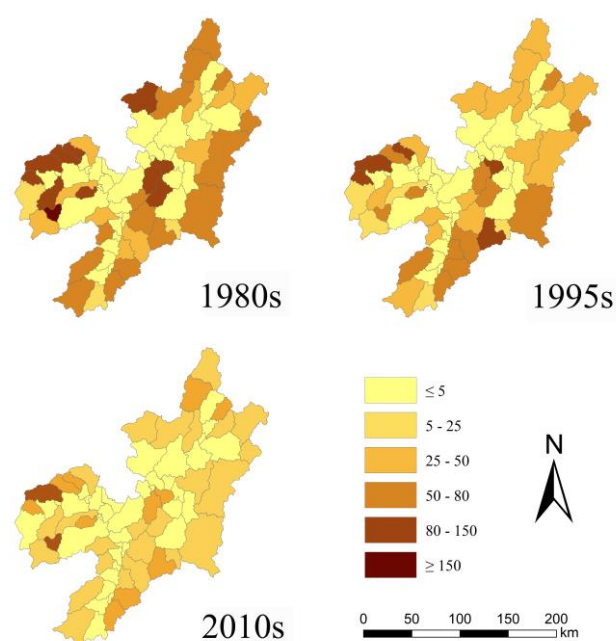


Figure 4. Sediment yield distribution of each sub-basin for the years 1980s, 1995s, and 2010s (t/ha/yr).

Table 4. Statistical analysis of the soil erosion and sediment yield for the upper Ganjiang Basin for the years 1980s, 1995s, and 2010s (t/ha/yr).

	Soil Erosion			Sediment Yield		
	P _{1980s}	P _{1995s}	P _{2010s}	P _{1980s}	P _{1995s}	P _{2010s}
Maximum	605.67	493.05	467.54	204.49	106.65	58.01
Minimum	13.8	7.85	5.34	0.68	0.78	0.60
Average	92.63	72.92	37.88	36.23	26.61	12.7
Standard Deviation	78.06	69.46	56.02	43.26	29.83	14.18

3.3. Correlation Analysis of Landscape Metrics in Different Combinations

As shown in Figure 5, overall, similar correlations were found between the parameters across the five combinations, although with some individual differences. Comparing all the combinations, similar correlations were found between the area metrics (i.e., PD, LPI, and AREA_MN). Specifically, PD was negatively correlated with LPI and AREA_MN, while there was a positive correlation between AREA_MN and LPI. For the fragmentation metrics (i.e., ED and ENN_MN), a negative correlation was found between them in Combination 1, Combination 3, and Combination 5, while no significant correlation was found between them in Combination 1 or Combination 4. For the shape metrics (i.e., LSI, SHAPE_MN, PARA_MN, and PAFRAC), their correlations differed considerably from combination to combination. Specifically, in Combination 1, LSI was positively correlated with PAFRAC and PARA_MN and was nonsignificantly correlated with SHAPE_MN; SHAPE_MN was significantly positively and negatively correlated with PAFRAC and PARA_MN, respectively; and PARA_MN was negatively correlated with PAFRAC. In Combination 2–Combination 5, similar correlations were found between the shape metrics. LSI was negatively correlated with SHAPE_MN and PAFRAC in Combination 2–Combination 5. LSI was similarly negatively correlated with PARA_MN in Combination 2 and Combination 4 but was nonsignificantly correlated with this metric in Combination 3 and Combination 5. Moreover, in Combination 2–Combination 5, SHAPE_MN was negatively correlated with PARA_MN and PAFRAC, while PARA_MN was positively correlated with PAFRAC. For the spatial structure metrics (i.e., CONTAG, IJI, DIVISION, SPLIT, and AI), in each combination, CONTAG was negatively correlated with IJI, DIVISION, and SPLIT and was positively correlated with AI. In each combination, IJI was negatively

correlated with AI and was positively correlated with DIVISION and SPLIT, although the correlation between IJI and DIVISION was nonsignificant in Combination 2 and Combination 4. For the evenness metrics (i.e., SHDI, SIDI, and SHEI), positive correlations were found between them in each combination.

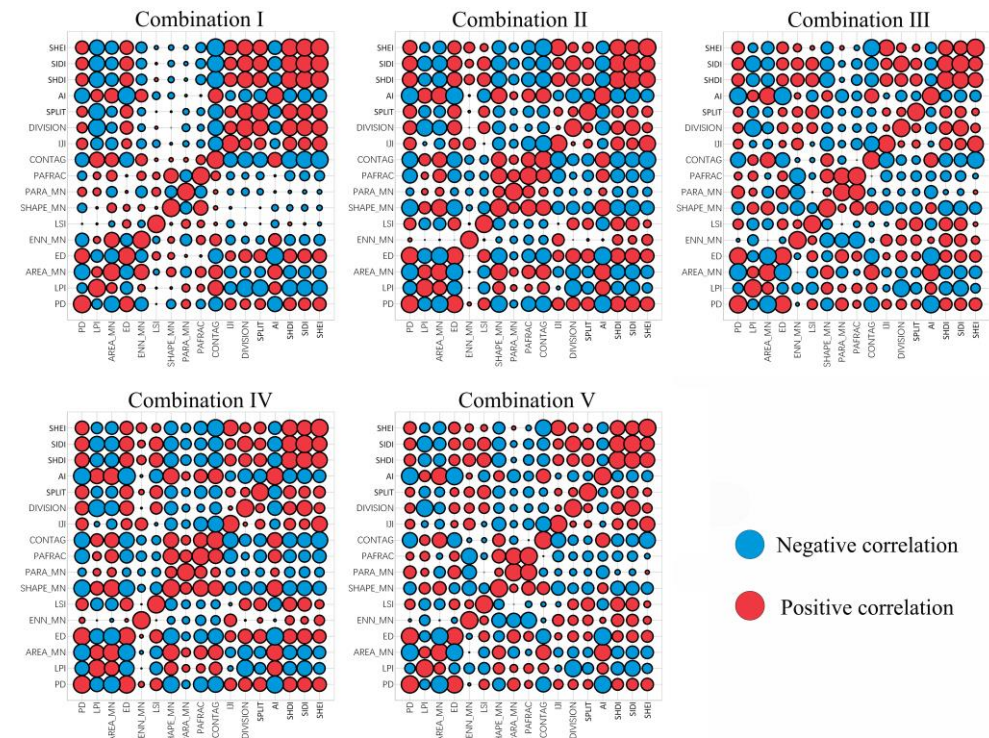


Figure 5. Correlation matrix of landscape metrics under five different combinations.

3.4. Correlation Analysis of the Soil Erosion and Landscape Metrics in Different Combinations

The correlations between the soil erosion and landscape metrics differed significantly from period to period and from combination to combination (Table 5). In Combination 1, soil erosion in P_{1995s} was positively correlated with PD, IJI, SHDI, SIDI, and SHEI and was negatively correlated with LPI and CONTAG, while the soil erosion in P_{2010s} was positively correlated with IJI, and SHEI was negatively correlated with CONTAG and was nonsignificantly correlated with the other metrics. In Combination 2, the soil erosion in P_{1980s} was negatively correlated with PD and ED and was positively correlated with AREA_MN and SHAPE_MN. The soil erosion in P_{1995s} was positively correlated with PAFRAC and AI and was negatively correlated with PD, ED, DIVISION, and SIDI. The soil erosion in P_{2010s} was positively correlated with AREA_MN, SHAPE_MN, PAFRAC, CONTAG, and AI; was negatively correlated with PD, ED, LSI, SHDI, and SIDI; and was nonsignificantly correlated with the other metrics. In Combination 3, the soil erosion in P_{1995s} was positively correlated with LPI, AREA_MN, SHAPE_MN, and AI and was negatively correlated with PD, ED, ENN_MN, LSI, DIVISION, SHDI, and SIDI. The soil erosion in P_{2010s} was positively correlated with SHAPE_MN and PAFRAC, was negatively correlated with SHDI and SIDI, and was nonsignificantly correlated with the other metrics. In Combination 4, the soil erosion in P_{1980s} was positively correlated with AREA_MN, SHAPE_MN, and AI and was negatively correlated with PD and ED. The soil erosion in P_{1995s} was positively correlated with LPI, AREA_MN, SHAPE_MN, and AI and was negatively correlated with PD, ED, and DIVISION. The soil erosion in P_{2010s} was positively correlated with AREA_MN, SHAPE_MN, PAFRAC, and AI; was negatively correlated with PD, ED, LSI, and DIVISION; and was nonsignificantly correlated with the other metrics. In Combination 5, the soil erosion in P_{1980s} was only positively correlated with SHAPE_MN. The soil erosion in P_{1995s} was positively correlated with LPI, AREA_MN, SHAPE_MN, and

AI and negatively correlated with PD, ED, ENN_MN, LSI, DIVISION, and SIDI. The soil erosion in P_{2010s} was positively correlated with SHAPE_MN and PAFRAC, was negatively correlated with ENN_MN, and was nonsignificantly correlated with the other metrics.

Table 5. The correlation between landscape metrics and soil erosion under five different combinations.

	Combination 1			Combination 2			Combination 3			Combination 4			Combination 5		
	P _{1980s}	P _{1995s}	P _{2010s}	P _{1980s}	P _{1995s}	P _{2010s}	P _{1980s}	P _{1995s}	P _{2010s}	P _{1980s}	P _{1995s}	P _{2010s}	P _{1980s}	P _{1995s}	P _{2010s}
PD	0.084	0.261 *	0.099	-0.270 *	-0.338 **	-0.343 **	-0.162	-0.269 *	-0.150	-0.285 *	-0.357 **	-0.356 **	-0.159	-0.269 *	-0.152
LPI	-0.130	-0.023 *	-0.180	0.111	0.225	0.146	0.189	0.392 **	0.200	0.177	0.308 **	0.197	0.167	0.395 **	0.212
AREA_MN	-0.090	-0.200	-0.117	0.379 **	0.406 **	0.410 **	0.187	0.390 **	0.154	0.388 **	0.421 **	0.418 **	0.184	0.389 **	0.159
ED	0.109	0.204	0.083	-0.276 *	-0.338 **	-0.335 **	-0.141	-0.316 **	-0.092	-0.303 **	-0.370 **	-0.354 **	-0.137	-0.316 **	-0.094
ENN_MN	-0.131	-0.145	-0.152	0.130	0.143	0.100	-0.119	-0.248 *	-0.218	0.080	0.139	-0.009	-0.150	-0.244 *	-0.258 *
LSI	-0.096	-0.166	-0.130	-0.182	-0.283 *	-0.232 *	-0.159	-0.269 *	-0.187	-0.185	-0.285 *	-0.233 *	-0.158	-0.269 *	-0.187
SHAPE_MN	-0.053	-0.098	-0.139	0.322 **	0.373 **	0.386 **	0.268 *	0.345 **	0.333 **	0.319 **	0.378 **	0.390 **	0.276 *	0.341 **	0.343 **
PARA_MN	-0.209	-0.128	-0.135	0.082	0.052	0.153	0.153	0.146	0.203	0.111	0.044	0.117	0.160	0.141	0.188
PAFRAC	0.003	-0.052	-0.061	0.174	0.237 *	0.264 *	0.199	0.220	0.275 *	0.175	0.212	0.259 *	0.206	0.220	0.270 *
CONTAG	-0.161	-0.252 *	-0.230 *	0.126	0.172	0.229 *	0.153	0.178	0.144	0.152	0.202	0.195	0.175	0.179	0.100
IJI	0.161	0.248 *	0.248 *	-0.017	-0.052	-0.100	-0.134	-0.042	-0.196	-0.030	-0.025 **	-0.065	-0.170	-0.042	-0.169
DIVISION	0.112	0.199	0.165	-0.214	-0.289 *	-0.224	-0.216	-0.387 **	-0.218	-0.237 *	-0.325 **	-0.247 *	-0.208	-0.383 **	-0.229
SPLIT	0.095	0.200	0.145	0.027	-0.060	-0.083	-0.053	-0.143	-0.127	-0.069	-0.139	-0.128	-0.039	-0.140	-0.129
AI	-0.112	-0.201	-0.081	0.280 *	0.357 **	0.334 **	0.143	0.330 **	0.092	0.314 **	0.391 **	0.358 **	0.147	0.335 **	0.100
SHDI	0.152	0.247 *	0.195	-0.139	-0.221	-0.240 *	-0.167	-0.261 *	-0.220 *	-0.074	-0.196	-0.146	-0.097	-0.228	-0.141
SIDI	0.161	0.246 *	0.203	-0.193	-0.262 *	-0.285 *	-0.225	-0.355 **	-0.271 *	-0.161	-0.272 *	-0.170	-0.195	-0.354 **	-0.176
SHEI	0.157	0.247 *	0.233 *	-0.041	-0.084	-0.155	-0.093	-0.100	-0.120	-0.036	-0.099	-0.063	-0.074	-0.097	-0.022

** and * indicate significant correlations at the 0.01 and 0.05 levels (two-tailed), respectively.

A comparison of the correlations between the soil erosion and each landscape metric in the five combinations shows that Combination 4 contained the most parameters significantly correlated with soil erosion at the 0.05 level, followed by Combination 2, Combination 3, and Combination 5 (Combination 3 = Combination 5), and Combination 1. Thus, the landscape metrics in Combination 4 were more strongly correlated with soil erosion in the sub-river basins.

3.5. Correlation Analysis of Sediment Yield and the Landscape Metrics in Different Combinations

Similarly, the relations between sediment yield and the landscape metrics differed significantly from period to period and from combination to combination (Table 6). In Combination 1, the sediment yield in P_{1980s} was positively correlated with LPI and CONTAG and was negatively correlated with ED, DIVISION, SPLIT, SHDI, SIDI, and SHEI. The sediment yield in P_{1995s} was positively correlated with LPI, PARA_MN, and CONTAG and was negatively correlated with IJI, DIVISION, SPLIT, SHDI, SIDI, and SHEI. The sediment yield in P_{2010s} was correlated with the landscape metrics in the same way as the sediment yield in P_{1995s}. In Combination 2, the sediment yield in P_{1980s} was positively correlated with PD, ED, ENN_MN, LSI, IJI, SPLIT, SHDI, SIDI, and SHEI and was negatively correlated with AREA_MN, SHAPE_MN, PARA_MN, PAFRAC, CONTAG, and AI. The relations between the sediment yield in each of P_{1995s} and P_{2010s} and the landscape metrics were similar those between the sediment yield in P_{1980s} and the landscape metrics. In Combination 3, the sediment yield in each of P_{1980s} and P_{2010s} was positively correlated with ENN_MN, SHDI, and SIDI and was negatively correlated with SHAPE_MN, PARA_MN, and PAFRAC. The sediment yield in P_{1995s} was correlated with more landscape metrics: positively with PD, ED, ENN_MN, LSI, IJI, SPLIT, SHDI, SIDI, and SHEI (similar to the sediment yield in P_{1995s} in Combination 2) and negatively with LPI, AREA_MN, SHAPE_MN, PAFRAC, CONTAG, and AI. In Combination 4, the sediment yield in each of the three periods was correlated with more landscape metrics in mostly similar ways: positively with PD, ED, ENN_MN, LSI, IJI, DIVISION, SPLIT, SHDI, SIDI, and SHEI and negatively with LPI, AREA_MN, SHAPE_MN, PARA_MN, PAFRAC, CONTAG, and AI. In Combination 5, the sediment yield in P_{1980s} was positively correlated with ENN_MN and SIDI and was negatively correlated with SHAPE_MN, PARA_MN, and PAFRAC. The sediment yield in P_{2010s} was positively correlated with ENN_MN, IJI, SHDI and SIDI and was negatively correlated with LPI, SHAPE_MN, PARA_MN, and PAFRAC. The sediment yield in P_{1995s} was correlated with the landscape metrics in ways similar to those in Combination 3. Overall, the correlations between sediment yield and each landscape metric in Combination 1 were mostly opposite to those in other combinations. For example, sediment yield was negatively correlated with the evenness metrics (i.e., SHDI, SIDI, and SHEI) in Combina-

tion 1 but was positively correlated with these metrics in the other combinations. Similar phenomena were observed for the area, fragmentation, shape, and spatial structure metrics. Thus, across all the combinations, there were highly similar correlations between the area metrics, between the evenness metrics, between the spatial structure metrics, and between the evenness metrics, while the correlations between the shape metrics in Combination 1 differed considerably from those in other combinations.

Table 6. The correlation between landscape metrics and sediment yield under five different combinations.

	Combination 1			Combination 2			Combination 3			Combination 4			Combination 5		
	P _{1980s}	P _{1995s}	P _{2010s}	P _{1980s}	P _{1995s}	P _{1980s}	P _{1995s}	P _{2010s}	P _{1980s}	P _{1995s}	P _{1980s}	P _{1995s}	P _{2010s}	P _{1980s}	P _{1995s}
PD	-0.174	-0.154	-0.135	0.400 **	0.415 **	0.422 **	-0.044	0.330 **	0.011	0.398 **	0.412 **	0.425 **	-0.045	0.328 **	0.008
LPI	0.463 **	0.498 **	0.518 **	-0.227	-0.262 *	-0.213	-0.227	-0.269 *	-0.240 *	-0.242 *	-0.277 *	-0.267 *	-0.218	-0.263 *	-0.241 *
AREA_MN	0.163	0.162	0.140	-0.345 **	-0.361 **	-0.353 **	0.004	-0.315 **	-0.043	-0.348 **	-0.363 **	-0.357 **	0.005	-0.313 **	-0.038
ED	-0.255 *	-0.183	-0.154	0.368 **	0.400 **	0.391 **	-0.091	0.308 **	-0.040	0.374 **	0.404 **	0.403 **	-0.091	0.307 **	-0.042
ENN_MN	0.049	0.077	0.020	0.256 *	0.170	0.206	0.450 **	0.350 **	0.424 **	0.267 *	0.157	0.190	0.467 **	0.351 **	0.414 **
LSI	0.048	0.138	0.090	0.236 *	0.303 **	0.239 *	0.141	0.278 *	0.142	0.234 *	0.301 **	0.239 *	0.141	0.278 *	0.142
SHAPE_MN	-0.100	-0.054	-0.046	-0.429 **	-0.399 **	-0.415 **	-0.358 **	-0.410 **	-0.366 **	-0.423 **	-0.400 **	-0.418 **	-0.354 **	-0.403 **	-0.365 **
PARA_MN	0.104	0.264 *	0.229 *	-0.315 **	-0.242 *	-0.248 *	-0.338 **	-0.116	-0.318 **	-0.318 **	-0.269 *	-0.275 *	-0.338 **	-0.122	-0.322 **
PAFRAC	0.101	0.030	0.039	-0.434 **	-0.377 **	-0.405 **	-0.432 **	-0.288 *	-0.420 **	-0.436 **	-0.367 **	-0.399 **	-0.434 **	-0.287 *	-0.419 **
CONTAG	0.333 **	0.344 **	0.324 **	-0.392 **	-0.421 **	-0.426 **	-0.027	-0.318 **	-0.110	-0.383 **	-0.431 **	-0.449 **	-0.024	-0.322 **	-0.090
IJI	-0.206	-0.274 *	-0.256 *	0.334 **	0.325 **	0.366 **	0.209	0.273 *	0.263 *	0.329 **	0.316 **	0.363 **	0.210	0.271 *	0.254 *
DIVISION	-0.450 **	-0.466 **	-0.494 **	0.221	0.237 *	0.211	0.189	0.209	0.197	0.222	0.241 *	0.229 *	0.186	0.205	0.195
SPLIT	-0.420 **	-0.445 **	-0.455 **	0.259 *	0.296 *	0.273 *	0.163	0.236 *	0.204	0.213	0.232 *	0.238 *	0.155	0.238 *	0.215
AI	0.263 *	0.193	0.166	-0.365 **	-0.402 **	-0.388 **	0.083	-0.306 **	0.034	-0.375 **	-0.404 **	-0.395 **	0.079	-0.306 **	0.038
SHDI	-0.310 **	-0.311 **	-0.314 **	0.402 **	0.428 **	0.408 **	0.275 *	0.436 **	0.300 **	0.310 **	0.410 **	0.394 **	0.210	0.418 **	0.303 **
SIDI	-0.312 **	-0.313 **	-0.310 **	0.361 **	0.386 **	0.357 **	0.263 *	0.378 **	0.284 *	0.330 **	0.384 **	0.372 **	0.251 *	0.373 **	0.283 *
SHEI	-0.325 **	-0.347 **	-0.329 **	0.365 **	0.398 **	0.392 **	0.089	0.327 **	0.157	0.325 **	0.413 **	0.408 **	0.067	0.342 **	0.165

** and * indicate significant correlations at the 0.01 and 0.05 levels (two-tailed), respectively.

A comparison of the correlations between sediment yield and each landscape metric in the five combinations shows that Combination 4 and Combination 2 both contained the most parameters significantly correlated with sediment yield at the 0.05 level, followed by Combination 1 and Combination 5 and Combination 3 (Combination 5 = Combination 3). Combination 4 contained the most parameters significantly correlated with sediment yield at the 0.01 level, followed by Combination 2 and Combination 3 (Combination 2 = Combination 3) and then Combination 5 and Combination 1 (Combination 5 = Combination 1). It can be concluded that the landscape metrics in Combination 4 were the most strongly correlated with sediment yield in the sub-river basins.

3.6. Quantification of the Correlations between Soil Erosion or Sediment Yield and Landscape Metrics

Since stronger correlations were found between the landscape metrics in Combination 4 and soil erosion and sediment yield, Combination 4 was selected in this study to establish PLSR models between the landscape metrics and the soil erosion and sediment yield of the sub-river basins within the upper Ganjiang Basin from the 1980s–2010s (Table 7). Q^2 is the ratio of the variances of the dependent variables (i.e., soil erosion and sediment yield) that can be explained by all the components of the PLSR models. The Q^2 values for all the PLSR models were above 0.5 except that for the soil erosion in P_{2010s}, whose Q^2 value was only 0.292, suggesting that the dependent variables could be well explained. Therefore, all the established PLSR models were robust.

Of the PLSR models for soil erosion, the PLSR model containing the first component for P_{1980s} explained 28% of the variance in soil erosion. The addition of the second component increased the explanatory ability of the PLSR model to 59.1%. From there, the addition of the third component and then the fourth component increased the explanatory ability of the PLSR model to 63% and 64.2%, respectively. Further adding components did not substantially increase the explanatory ability of the PLSR model for the dependent variable. In total, the PLSR models for P_{1995s} and P_{2010s} explained 61% and 41.2% of the variance in soil erosion, respectively.

Table 7. Summary of the PLSR models of soil erosion and sediment yield under Combination 4.

Response Variable Y	Year	R ²	Q ²	Component	% of Explained Variability in Y	Cumulative Explained Variability in Y (%)	Q ² _{cum}	RMSECV (t/ha/yr)
Soil erosion	1980s	0.59	0.57	1	28.00	28.00	0.26	98.88
				2	31.00	59.10	0.57	74.98
				3	3.89	63.00	0.58	75.13
				4	1.24	64.20	0.53	78.67
	1995s	0.60	0.55	1	21.30	21.30	0.20	88.54
				2	31.90	53.20	0.51	69.14
				3	6.48	59.70	0.55	66.98
				4	1.28	61.00	0.52	68.92
	2010s	0.39	0.29	1	11.40	11.40	0.11	62.79
				2	20.60	31.90	0.29	55.92
				3	7.32	39.30	0.29	55.98
				4	1.92	41.20	0.25	57.36
Sediment yield	1980s	0.56	0.49	1	33.70	33.70	0.30	47.85
				2	11.40	45.10	0.41	43.60
				3	8.71	53.80	0.48	40.77
				4	1.95	55.80	0.49	40.51
	1995s	0.58	0.52	1	36.30	36.30	0.31	33.45
				2	12.40	48.60	0.44	30.10
				3	7.39	56.00	0.51	28.09
				4	1.88	57.90	0.52	27.75
	2010s	0.57	0.51	1	37.00	37.00	0.33	15.75
				2	11.90	48.90	0.45	14.25
				3	6.57	55.50	0.51	13.44
				4	1.66	57.10	0.51	13.31

Of the PLSR models for sediment yield, the PLSR model containing the first component for P_{1980s} explained 33.7% of the variance in sediment yield. The addition of the second component increased the explanatory ability of the PLSR model to 45.1%. From there, the addition of the third component and then the fourth component increased the explanatory ability of the PLSR model to 53.8% and 55.8%, respectively. Further adding components did not substantially increase the explanatory ability of the PLSR model for the dependent variable. In total, the PLSR models for P_{1995s} and P_{2010s} explained 57.9% and 57.1% of the variance in sediment yield, respectively. The minimum RMSECV for each PLSR model corresponded to the maximum Q², suggesting that the model was optimal.

Redundant variables may reduce the statistical significance of a PLSR model, so it is necessary to further evaluate the importance of each landscape metric to generate optimal PLSR models. The relative importance of an LR metric can be measured by its VIP score. The key metrics affecting the soil erosion and sediment yield in P_{1980s}, P_{1995s}, and P_{2010s} were highly similar (Table 8). SPLIT, PARA_MN, ENN_MN, ED, and LSI were the landscape metrics with the highest VIP scores. The VIP scores of SPLIT and PARA_MN for soil erosion and sediment yield in all the periods were greater than 1. The VIP scores of ENN_MN were greater than 1 for the soil erosion in P_{1980s} and P_{1995s} and the sediment yield in P_{1980s} and were close to 1 in the other combinations. The VIP scores of ED were greater than 1 for the soil erosion and sediment yield in P_{2010s} and were close to 1 in the other combinations. The VIP scores of LSI were greater than 1 for the soil erosion and sediment yield in P_{1995s} and the soil erosion in P_{2010s} and were close to 1 in the other combinations. These findings show that these five landscape metrics play main roles in controlling soil erosion and sediment yield in the river basin and thus can be used as the main metrics for establishing optimal PLSR models for each stage.

Table 8. The VIP of landscape metrics for soil erosion and sediment yield under Combination 4.

	Soil Erosion			Sediment Yield		
	1980s	1995s	2010s	1980s	1995s	2010s
SPLIT	20.745	20.528	20.315	30.116	30.181	30.230
PARA_MN	20.555	20.603	20.539	10.894	10.873	10.863
ENN_MN	10.046	10.149	0.998	10.126	0.903	0.890
ED	0.915	0.983	10.320	0.995	0.981	10.018
LSI	0.794	10.037	10.291	0.990	10.072	0.883
PD	0.442	0.510	0.757	0.580	0.549	0.589
AI	0.301	0.327	0.347	0.218	0.223	0.224
CONTAG	0.208	0.220	0.214	0.179	0.200	0.191
IJI	0.192	0.199	0.190	0.205	0.211	0.207
LPI	0.074	0.130	0.116	0.095	0.100	0.098
AREA_MN	0.025	0.027	0.041	0.019	0.018	0.019
SHDI	0.016	0.017	0.021	0.019	0.024	0.023
PAFRAC	0.005	0.005	0.005	0.003	0.003	0.003
SHAPE_MN	0.005	0.005	0.005	0.003	0.003	0.003
DIVISION	0.004	0.004	0.004	0.003	0.003	0.003
SIDI	0.003	0.004	0.003	0.003	0.003	0.003
SHEI	0.002	0.003	0.003	0.002	0.003	0.003

A PLSR analysis in the study area in all three study periods yielded the following quantitative relationships between soil erosion (Q_{SE}) and sediment yield (Q_{SY}) in the river basin and the landscape metrics:

$$Q_{SE} = -10.016X_{ED} - 0.155X_{LSI} + 0.203X_{PARA_MN} + 0.390X_{ENN_MN} + 0.005X_{SPLIT} \quad (1)$$

$$Q_{SY} = 0.385X_{ED} + 0.060X_{LSI} - 0.194X_{PARA_MN} + 0.315X_{ENN_MN} - 0.001X_{SPLIT} \quad (2)$$

The Q^2 values for soil erosion and sediment yield are 0.51 and 0.47, respectively, suggesting that the models have good predictive ability and robustness.

4. Discussion

Of all the land-use types in the upper Ganjiang Basin in the 1980s–2010s, other wooded lands increased in area by the greatest percentage, followed by construction lands, dry lands, forests, and water bodies, while open forests shrank by the greatest percentage, followed by shrublands. This phenomenon may have been a result of economic development and human activity in the region [25]. Economic development led to a considerable increase in the urban construction land area. Large-scale prevention and control measures have been implemented to prevent severe soil erosion since the 1990s. Extensive cultivation of pioneer tree species (e.g., *Pinus massoniana*) for water and soil conservation in areas with low vegetation coverage resulted in a rapid increase in the local area of local shrublands. Later, some of these lands underwent succession and became forests with high coverage, some were turned into urban construction lands, and some were developed into economic forests (e.g., navel orange orchards and tea plantations), leading to a rapid expansion of other wooded lands. In contrast, there was a continuous decrease in open forests. Similarly, the evolution and succession of open forests resulted in notable increases in the areas of economic forests and construction lands. The expansion of dry lands may have been a result of the discontinuation of farming in some orchards and farmlands due to the migration of local farmers to urban areas for work. The increase in the area of water bodies may have only been related to the interannual variation in rainfall. The overall significant decreases in soil erosion and sediment yield in the river basin reflect the considerable importance attached by the local authorities to water and soil conservation as well as the marked results of the soil erosion control measures.

The inherent defects of the SWAT model prevent it from accurately simulating long-term soil erosion conditions [31]. In addition, the soil erosion module used in the SWAT

model is an empirical model, whereas the actual factors affecting soil erosion and sediment yield and their processes are much more complex than model simulations. As a result, the SWAT model may not be able to yield simulations completely consistent with the actual situation. But this is a common, objective problem facing model simulations and is not within the scope of this study. Under current circumstances, collecting soil erosion measurements at a river basin scale is an exceedingly difficult task. It is easier to measure the runoff and sediment discharge in a river at the outlet of the river basin. Therefore, in the presence of limited data, the powerful simulation and calibration tools of the SWAT model can be employed to effectively evaluate soil erosion conditions within a river basin and to provide a basis for formulating relevant policies [9].

It is suggested that there are three types of landscape structures: patches, corridors, and matrix [1]. The landscape matrix is the largest and most connected type of landscape element in the landscape, and as such, it can potentially have a great influence on the dynamics of the species in the landscape [9]. However, constrained by the characteristics of the landscape matrix and the complexity of ecological processes, reliance on the landscape matrix is often criticized for failing to accurately reflect landscape characteristics and their ecological relevance [40]. How to link landscape metrics to specific ecological processes or develop new landscape indicators is one of the current challenges in landscape ecology research [15]. Many scholars have conducted active explorations for this purpose. For example, the gradient paradigm is combined with the landscape pattern index to analyze the landscape pattern characteristics of sample strips or local areas [41]. The directional infiltration index (DLI) is used to characterize the ability of landscape cover to hold back water and soil [3]. These studies have incorporated some theoretical paradigms and landscape patterns into landscape metrics, which have given new dynamics to landscape pattern analysis. However, due to the complexity of ecological processes, the multiplicity of influencing factors and their variability at any spatial and temporal scales, these new metrics still face many doubts and difficulties in the analysis of pattern–process interrelationships. Therefore, this study presents a new landscape indicator and explores the relationship between landscape metrics and soil erosion and sediment yield at larger scales. The results show that compared to land use alone, the addition of the LS, K, R, and C factors significantly altered the landscape pattern in the river basin but did not lead to significant changes in the correlations between most of the landscape metrics, which reflects their relatively deterministic mathematical relations [42].

A comparison of the five combinations of landscape metrics shows that the landscape metrics in Combination 2 were more significantly correlated with the soil erosion and sediment yield in the river basin than those in Combination 1, suggesting that the addition of the relatively fixed LS and K factors can effectively improve the explanatory ability of the landscape metrics for soil erosion and sediment yield. An analysis of Combination 3 and Combination 4, which in addition to the Combination 2 factors had dynamically varying C and R factors, respectively, shows that adding the R factor caused the correlations between the landscape metrics and the soil erosion and sediment yield to further increase to their highest levels, which also reflects the importance of R to the soil erosion and sediment yield process. In contrast, the addition of C weakened the correlations. This may be because the land use itself reflects certain vegetation cover conditions, while adding C, which varies relatively significantly at seasonal and annual scales, results in a certain degree of information redundancy, thereby interfering with the ability of the PLSR model to explain and predict soil erosion and sediment yield. This explanation is corroborated by the similarly weak correlations between each landscape metric of Combination 5 and soil erosion and sediment yield.

The results of this study showed that the landscape pattern had a significant influence on the soil erosion and sediment yield in the upper Ganjiang Basin. The PLSR model was able to identify the main landscape metrics controlling soil erosion and sediment yield in each sub-basin of the upper Ganjiang Basin. All landscape metrics can be obtained relatively easily through land-use maps, DEM, etc. Therefore, in the absence of sufficient

actual monitoring data, soil erosion and sediment yield in the basin can still be predicted with reasonable accuracy through the new landscape indicator. However, the quantitative relationships of the new landscape indicator with soil erosion and sediment yield in the basin that we established in this study have limitations. These quantitative relationships may be applicable only to the study area and the periods involved in this study and are not universal. There are doubts about the ecological correlations of landscape metrics [43,44]. In addition, landscape metrics are unable to reflect soil erosion and sediment yield processes [45]. While statistically significant correlations were found between the landscape metrics and between these metrics and soil erosion and sediment yield, relevant principles and mechanisms of action remain unclear and require further exploration.

5. Conclusions

This paper presents a case study of the upper Ganjiang Basin. Five combinations of landscape metrics were chosen for analysis. Through simulations using a hydrological model and PLSR, the correlations between the landscape metrics and between the landscape metrics and the soil erosion and sediment yield of the river basin were investigated. The main conclusions are drawn as follows:

- (1) In the 1980s–2010s, the areas of other wooded lands and construction lands in the upper Ganjiang Basin increased to large degrees, which was related to economic factors such as urban expansion, afforestation, and extensive development of economic forests. This period also saw considerable decreases in the soil erosion and sediment yield of the river basin, reflecting the great importance attached by the local authorities to water and soil conservation efforts that effectively restored the ecological environment.
- (2) Five combinations were established through the addition of the relatively fixed soil erosion factors (i.e., the LS and K factors) and/or one or both of the dynamically varying C and R factors to the land-use. The correlations between the landscape metrics in each combination were calculated. When we compared the correlations between the landscape metrics across the five combinations, highly similar correlations were found between the area metrics, between the fragmentation metrics, between the spatial structure metrics, and between the evenness metrics in the different combinations. However, the correlations between the shape metrics in Combination 1 differed considerably from those in the other combinations.
- (3) Comparison of the correlations between the landscape metrics in different combinations and the soil erosion and sediment yield of the river basin showed that the landscape metrics in Combination 4, which combined the land-use and the LS, K, and R factors, were the most significantly correlated with soil erosion and sediment yield. The correlations between the landscape metrics with the highest VIP scores in Combination 4 and the soil erosion and sediment yield in the river basin were quantified. This study explores a new indicator for the correlations between landscape metrics and soil erosion and sediment yield and provides decision-makers with a new quantification method for evaluating these correlations and formulating water and soil conservation policies. While we attempted to explain why the landscape indicator in Combination 4 were the most significantly correlated with the soil erosion and sediment yield in the river basin, further research is needed to determine the relevant internal principles and mechanisms of action from a landscape pattern perspective.

Author Contributions: Y.Z. performed the data compilation, simulations, and analysis and drafted the manuscript. C.T. and S.Z. contributed to the conception of the study. N.W., Y.S., K.L. and X.N. helped revise the manuscript. All authors have read and agreed to the published version of the manuscript.

Funding: This research was jointly funded by the National Key Research and Development Program of China (No. 2019YFC1510503), the National Natural Science Foundation of China (No. 41867016), the Natural Science Foundation of Jiangxi Province (No. 20202BABL203029), the Postdoctoral

Research Merit Foundation of Jiangxi Province (No. 2019KY46), and the Water Conservancy Science and Technology Project of Jiangxi Province (Nos. 201922ZDKT17, 201821ZDKT15, 202124ZDKT25, 202124ZDKT24, 201821ZDKT18, 201922ZDKT08, 202123TGKT07, and 201921TGKT12).

Institutional Review Board Statement: Not applicable.

Informed Consent Statement: Not applicable.

Data Availability Statement: Not applicable.

Conflicts of Interest: The authors declare no conflict of interest.

References

1. Forman, R.T.T. *Land Mosaics: The Ecology of Landscapes and Regions*; Cambridge University Press: Cambridge, UK, 1995.
2. Turner, M.G. Landscape Ecology: The Effect of Pattern on Process. *Annu. Rev. Ecol. Syst.* **1989**, *20*, 171–197. [[CrossRef](#)]
3. Ludwig, J.A.; Bastin, G.N.; Chewings, V.H.; Eager, R.W.; Liedloff, A.C. Leakiness: A new index for monitoring the health of arid and semiarid landscapes using remotely sensed vegetation cover and elevation data. *Ecol. Indic.* **2007**, *7*, 442–454. [[CrossRef](#)]
4. Huang, Z.; Tian, Y.; Xiao, W.; Ma, D. Effects of landscape patterns on runoff and sediment export from typical agroforestry watersheds in the Three Gorges Reservoir area, China. *Acta Ecol. Sin.* **2013**, *33*, 7487–7495. [[CrossRef](#)]
5. Wei, O.; Skidmore, A.K.; Hao, F.; Wang, T. Soil erosion dynamics response to landscape pattern. *Sci. Total Environ.* **2010**, *408*, 1358–1366.
6. Fu, B.-J.; Wang, Y.; Lu, Y.; He, C.; Chen, L.-D.; Song, C.-J. The effects of land-use combinations on soil erosion: A case study in the Loess Plateau of China. *Prog. Phys. Geogr.* **2009**, *33*, 793–804. [[CrossRef](#)]
7. Liu, Y.; Lü, Y.; Fu, B.-J. Implication and limitation of landscape metrics in delineating relationship between landscape pattern and soil erosion. *Acta Ecol. Sin.* **2011**, *31*, 267–275.
8. Hulshoff, R.M. Landscape indices describing a Dutch landscape. *Landsc. Ecol.* **1995**, *10*, 101–111. [[CrossRef](#)]
9. Shi, Z.H.; Ai, L.; Li, X.; Huang, X.D.; Wu, G.L.; Liao, W. Partial least-squares regression for linking land-cover patterns to soil erosion and sediment yield in watersheds. *J. Hydrol.* **2013**, *498*, 165–176. [[CrossRef](#)]
10. Dash, C.B.; Fraterrigo, J.M.; Hu, F.S. Land cover influences boreal-forest fire responses to climate change: Geospatial analysis of historical records from Alaska. *Landsc. Ecol.* **2016**, *31*, 1781–1793. [[CrossRef](#)]
11. Venne, L.S.; Tsai, J.S.; Cox, S.B.; Smith, L.M.; Mcmurry, S.T. Amphibian Community Richness in Cropland and Grassland Playas in the Southern High Plains, USA. *Wetlands* **2012**, *32*, 619–629. [[CrossRef](#)]
12. Zheng, C.; Zhi, F.X.; Lei, W. Landscape Structure Analysis of Xiao’shao Reclaimed Area Based on Remote Sensing Image. *Remote Sens. Inf.* **2003**, *4*, 28–32.
13. Shehab, Z.N.; Jamil, N.R.; Aris, A.Z.; Shafie, N.S. Spatial variation impact of landscape patterns and land use on water quality across an urbanized watershed in Bentong, Malaysia. *Ecol. Indic.* **2021**, *122*, 107254. [[CrossRef](#)]
14. Boongaling, C.G.K.; Faustino-Eslava, D.V.; Lansigan, F.P. Modeling land use change impacts on hydrology and the use of landscape metrics as tools for watershed management: The case of an ungauged catchment in the Philippines. *Land Use Policy* **2018**, *72*, 116–128. [[CrossRef](#)]
15. Wang, J.; Yang, L.; Wei, W.; Chen, L.; Huang, Z. Effects of landscape pattern on watershed soil erosion and sediment delivery in hilly and gully region of the Loess Plateau of China: Patch class-level. *Acta Ecol. Sin.* **2011**, *31*, 5739–5748.
16. Corry, R.C.; Nassauer, J.I. Limitations of using landscape pattern indices to evaluate the ecological consequences of alternative plans and designs. *Landsc. Urban Plan.* **2005**, *72*, 265–280. [[CrossRef](#)]
17. Yan, B.; Fang, N.F.; Zhang, P.C.; Shi, Z.H. Impacts of land use change on watershed streamflow and sediment yield: An assessment using hydrologic modelling and partial least squares regression. *J. Hydrol.* **2013**, *484*, 26–37. [[CrossRef](#)]
18. Carrascal, L.M.; Galván, I.; Gordo, O. Partial least squares regression as an alternative to current regression methods used in ecology. *Oikos* **2009**, *118*, 681–690. [[CrossRef](#)]
19. Renard, K.; Foster, G.; Weesies, G.; McCool, D.; Yoder, D. Predicting soil erosion by water: A guide to conservation planning with the Revised Universal Soil Loss Equation (RUSLE). *Agric. Handb.* **1996**, *703*, 25–28.
20. Yao, X.; Yu, J.; Jiang, H.; Sun, W.; Li, Z. Roles of soil erodibility, rainfall erosivity and land use in affecting soil erosion at the basin scale. *Agric. Water Manag.* **2016**, *174*, 82–92. [[CrossRef](#)]
21. Wang, B.; Zheng, F.; Römkens, M.J.M. Comparison of soil erodibility factors in USLE, RUSLE2, EPIC and Dg models based on a Chinese soil erodibility database. *Acta Agric. Scand. Sect. B—Soil Plant Sci.* **2013**, *63*, 69–79. [[CrossRef](#)]
22. Khaleghpanah, N.; Shorafa, M.; Asadi, H.; Gorji, M.; Davari, M. Modeling soil loss at plot scale with EUROSEM and RUSLE2 at stony soils of Khamesan watershed, Iran. *Catena* **2016**, *147*, 773–788. [[CrossRef](#)]
23. Sun, W.; Shao, Q.; Liu, J.; Zhai, J. Assessing the effects of land use and topography on soil erosion on the Loess Plateau in China. *Catena* **2014**, *121*, 151–163. [[CrossRef](#)]
24. Guo, L.P.; Mu, X.M.; Hu, J.M.; Gao, P.; Zhang, Y.F.; Liao, K.T.; Bai, H.; Chen, X.L.; Song, Y.J.; Jin, N.; et al. Assessing Impacts of Climate Change and Human Activities on Streamflow and Sediment Discharge in the Ganjiang River Basin (1964–2013). *Water* **2019**, *11*, 1679. [[CrossRef](#)]

25. Zheng, H.; Fang, S.; Yang, J.; Xie, S.; Chen, X. Analysis on Evolution Characteristics and Impacting Factors of Annual Runoff and Sediment in the Ganjiang River During 1970–2009. *J. Soil Water Conserv.* **2012**, *26*, 28–32.
26. Fu, Q.L.; Deng, Y.L.; Hu, H.Q.; Yu, X.; Wan, T.Y.; Han, X.F. Sorption of the toxin of *Bacillus thuringiensis* subsp. *kurstaki* by soils: Effects of iron and aluminium oxides. *Eur. J. Soil Sci.* **2012**, *63*, 565–570. [[CrossRef](#)]
27. Zhang, Y.; Tang, C.; Ye, A.; Zheng, T.; Nie, X.; Tu, A.; Zhu, H.; Zhang, S. Impacts of Climate and Land-Use Change on Blue and Green Water: A Case Study of the Upper Ganjiang River Basin, China. *Water* **2020**, *12*, 2661. [[CrossRef](#)]
28. Torabi Haghghi, A.; Darabi, H.; Shahedi, K.; Solaimani, K.; Kløve, B. A Scenario-Based Approach for Assessing the Hydrological Impacts of Land Use and Climate Change in the Marboreh Watershed, Iran. *Environ. Model. Assess.* **2019**, *25*, 41–57. [[CrossRef](#)]
29. Shi, P.; Zhang, Y.; Ren, Z.; Yu, Y.; Li, P.; Gong, J. Land-use changes and check dams reducing runoff and sediment yield on the Loess Plateau of China. *Sci. Total Environ.* **2019**, *664*, 984–994. [[CrossRef](#)] [[PubMed](#)]
30. Abbaspour, K.C.; Rouholahnejad Freund, E.; Ashraf Vaghefi, S.; Srinivasan, R.; Yang, H.; Kløve, B. A continental-scale hydrology and water quality model for Europe: Calibration and uncertainty of a high-resolution large-scale SWAT model. *J. Hydrol.* **2015**, *524*, 733–752. [[CrossRef](#)]
31. Neitsch, S.L.; Arnold, J.G.; Kiniry, J.R.; Srinivasan, R.; Williams, J.R. Soil and water assessment tool user’s manual. In *GSWRL Report, Version 2000*; TWRI Report TR-192; Texas Water Resources Institute: College Station, TX, USA, 2002; Volume 202.
32. Gassman, P.; Reyes, M.; Green, C.; Arnold, J. The soil and water assessment tool: Historical development, applications, and future research directions. *Trans. ASABE* **2007**, *50*, 1211–1250. [[CrossRef](#)]
33. Cuceloglu, G.; Abbaspour, K.; Ozturk, I. Assessing the Water-Resources Potential of Istanbul by Using a Soil and Water Assessment Tool (SWAT) Hydrological Model. *Water* **2017**, *9*, 814. [[CrossRef](#)]
34. Abbaspour, K.; Vejdani, M.; Haghghat, S. *SWAT-CUP Calibration and Uncertainty Programs for SWAT*; Modelling and Simulation Society of Australia and New Zealand: Christchurch, New Zealand, 2007; pp. 1596–1602.
35. Gupta, H.; Kling, H.; Yilmaz, K.; Martinez, G. Decomposition of the Mean Squared Error and NSE Performance Criteria: Implications for Improving Hydrological Modelling. *J. Hydrol.* **2009**, *377*, 80–91. [[CrossRef](#)]
36. Abdi, H. Partial least squares regression and projection on latent structure regression (PLS Regression). *WIREs Comput. Stat.* **2010**, *2*, 97–106. [[CrossRef](#)]
37. Wang, B.; Fang, S.; Yang, Q. Acquisition Method of Evaluation Model of Soil and Water Loss and Its Affecting Factors of the Southern Jiangxi. *Soil Water Conserv. China* **2011**, *12*, 16–19.
38. McGarigal, K.; Cushman, S.A.; Neel, M.C.; Ene, E. FRAGSTATS: Spatial Pattern Analysis Program for Categorical Maps. Computer Software Program Produced by the Authors at the University of Massachusetts Amherst. 2002. Available online: <https://www.umass.edu/landeco/research/fragstats/fragstats.html> (accessed on 7 June 2021).
39. McGarigal, K.; Marks, B.J. *FRAGSTATS: Spatial Pattern Analysis Program for Quantifying Landscape Structure*; Gen. Tech. Rep. PNW-GTR-351; Department of Agriculture, Forest Service, Pacific Northwest Research Station: Portland, OR, USA, 1995.
40. Chen, L.; Liu, Y.; Lü, Y.; Feng, X.; Fu, B. Landscape pattern analysis in landscape ecology: Current, challenges and future. *Acta Ecol. Sin.* **2008**, *28*, 5521–5531.
41. Luck, M.; Wu, J. A gradient analysis of urban landscape pattern: A case study from the Phoenix metropolitan region, Arizona, USA. *Landsc. Ecol.* **2002**, *17*, 327–339. [[CrossRef](#)]
42. Chaoyue, L.I.; Fang, H.; Conservation, W. Simulation of Sediment Yield and Analysis of Influencing Factors in the Shouchang River Basin Based on SWAT Model. *J. Soil Water Conserv.* **2019**, *33*, 127–135.
43. Tischendorf, L. Can landscape indices predict ecological processes consistently? *Landsc. Ecol.* **2001**, *16*, 235–254. [[CrossRef](#)]
44. Harbin, L.; Wu, J. Use and misuse of landscape indices. *Landsc. Ecol.* **2003**, *19*, 389–399.
45. Lin, M.-L.; Cao, Y.; Wang, S. Limitations of landscape pattern analysis based on landscape indices: A case study of Lizejian wetland in Yilan of Taiwan Province, China. *J. Appl. Ecol.* **2008**, *19*, 139–143.